A Model for the Analysis of the Structural Failure of the Clay Core in Rockfill Dams Due to Overtopping

L.F. Ricoy, M.Á. Toledo and R. Morán
Department of Civil Engineering: Hydraulics, Energy and Environment
Dam Safety Research Group (SERPA)
Technical University of Madrid (UPM)
Spain
E-mail: lucas.fricoy@alumnos.upm.es

ABSTRACT

In 2014 the Dam Safety Research Group (SERPA) of the Technical University of Madrid performed several tests to assess the behavior of rockfill dams in overtopping scenarios. A structural failure pattern of the clay core was observed, as expected. Hence, it was concluded that a model to simulate the observed failure mechanisms was needed. The model described herein provides the first results on assessment of the clay core stability following failure of the downstream shell. The failure process may result in one or more brittle and abrupt breakage phases of the core, herein classified as structural breakages, as opposed to the progressive failure caused by the erosion of the cohesive material. Thus, total or partial failure of the clay core occurs when the acting forces reach one of the instability conditions: overturning or sliding. The model was utilized to retroactively analyze two experiments carried out in the laboratory; the results obtained were consistent with the experimental measurements. The model is based on simple mechanical principles, but represents a paradigm shift in the interpretation and evaluation of the overtopping failure processes, especially since it results in a failure hydrograph different from those typically adopted, and therefore, has repercussions in the development of emergency plans.

Keywords: Dam failure, overtopping, rockfill dam, clay core.

1. INTRODUCTION

After the advent of geotechnics and its consolidation as a science, filters and drain criteria, together with slope equilibrium limit analysis, established themselves as fundamental parameters for the evaluation of the stability of embankment dams. However, this traditional approach may not be sufficient when embankment dams are subject to exceptional situations, as in the case of overtopping. Currently, the most widespread perspective is that, in central core rockfill dams, overtopping flows induce a progressive failure process caused by the erosion of the core. However, this may not be the most likely process resulting in failure. In rockfill dams, the percolation of water through the downstream shell results in mass sliding and particle dragging, which quickly leaves the core partially unsupported (Toledo, 1997) (Figure 1).
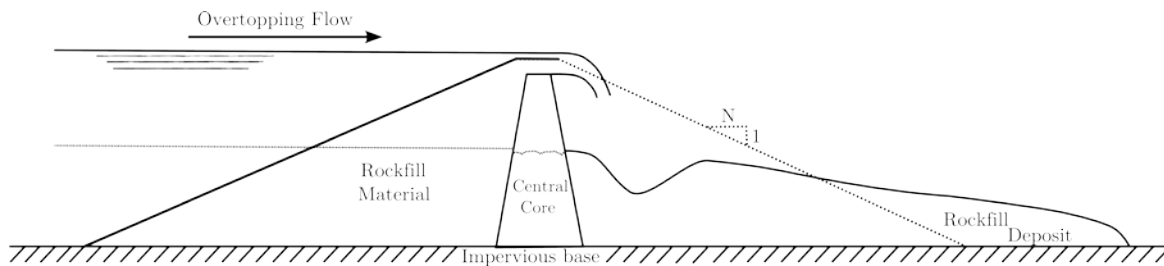

Figure 1: Failure of rockfill downstream slope during an overtopping episode. Source: Toledo et al. (2014).

The partial failure of the rockfill shell, although necessary for the development of the breakage, is generally not considered sufficient to cause a breach of the dam with uncontrolled release of stored water. After the loss of a shell section, the core would be subjected to new system forces and should resist as a gravity wall without support until the failure occurs, and if failure occurs, rupture is of a structural type. This breach mechanism was also described by Odendaal & Van Zyl (1979) in the report of the failure of the Hans Strydom cofferdam. To test the validity of this understanding, the Dam Safety Research Group of the Technical University of Madrid (SERPA) performed laboratory trials on two rockfill dam prototypes with a central core, which were subject to overtopping (Toledo, et al. 2015). The experiments showed that the failure process evolved in the assumed way (at laboratory size), culminating in a brittle and abrupt failure of the dam core. Something similar also happened in the case of a test of an upstream faced rockfill dam prototype.

Based upon the results of these trials, a simple model was developed to evaluate the stability of the core after the partial or complete loss of the downstream rockfill shell. Provided the assumptions are sufficiently adequate, the model allows the estimation of the structural breach size, providing a basis for a more realistic quantification of the failure hydrograph, valuable for the development of a more realistic analysis and development of an emergency plan. It should be noted that overtopping is the main cause responsible for embankment dam failures [30% according to Costa, (1995) *apud* Wu et al. (2011)] and emergency procedures consider this scenario. Additionally, the predominant methodology in use today, based upon the gradual evolution of the breach by erosion, can sometimes predict failure waves that are smoother than expected in the field, which would be non-conservative (Toledo, et al. 2014).

2. THE MODEL

In order to evaluate the stability of the core after the loss of the downstream shell, a simplified calculation model based upon the theory of static equilibrium was adopted with the following assumptions: linear elastic behavior, and a system of small displacements and small deformations where the flat sections remain flat (Bernoulli-Navier hypothesis). As shown previously, the method analyzed and presented is a refined approach based upon criteria similar to those adopted in the evaluation of the stability of retaining wall systems. Broich et al. (2005) adopted a model for dam breaches based upon a similar philosophy. Indeed, this analysis incorporated several assumptions presented by Broich et al. (2005), with the aim of continually elaborating and advancing the most robust possible model.

2.1. Destabilizing Forces

The primary action responsible for inducing a failure of the core is the pressure of the water in the reservoir. When dealing with an overtopping situation, a simplification is to assume that overflow occurs continuously over the crest and, therefore, generates a trapezoidal diagram of hydrostatic pressure. The top of the core is assumed to be perfectly regular, in such a way that the height of the water column is the same along the entire width (Figure 2).
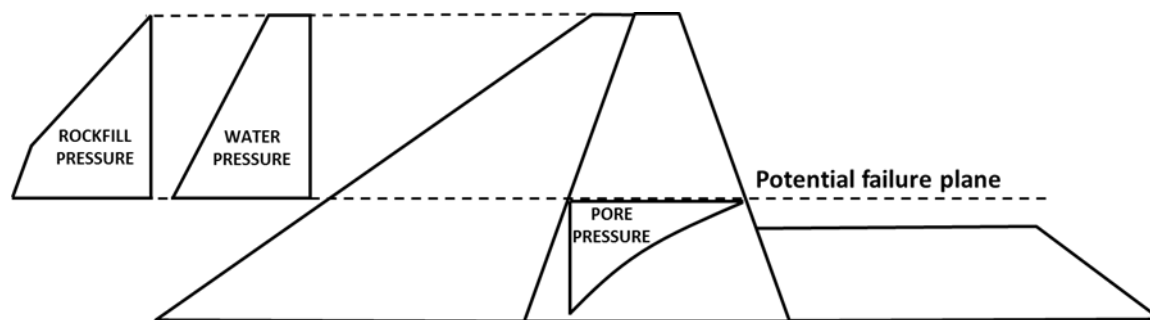

Figure 2: Pressures applied on the core, above a potential failure plane.

The core is also subject to lateral pressure caused by the upstream rockfill and, unlike the hydrostatic pressure, the load applied is triangular. After the erosion of the downstream shell, all of the rockfill above the core crest loses its support and is carried into the water below. Three different loading cases can be predicted (Figure 3).
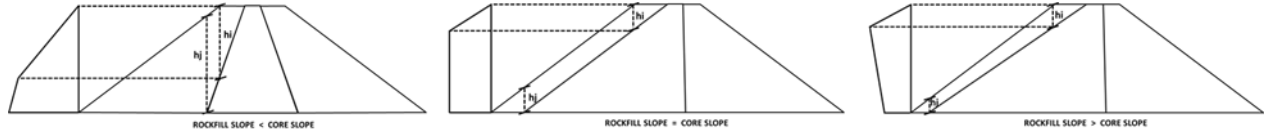

Figure 3: Variation of rockfill pressure on the core as a function of core slope. Left section is the usual configuration, and centre and right sections are not expected in practice.

For the determination of the rockfill thrust, the coefficient of lateral pressure was calculated by Jaky's formula:

$$K = 1 - \sin \varphi_r \tag{1}$$

where φ_r is the internal friction angle of the rockfill.

Another important force contributing to the overturning moment is pore water pressure. Like all of the other elements involved in this problem, pore pressure values vary for different horizontal sections of the core (potential failure planes). Bearing in mind that storm durations and flood surcharge in reservoirs may occur during a period of hours, this rapid rise in the pool elevation in the reservoir does not produce a change of the phreatic line level. For this reason, the pore pressure was considered constant throughout the process.

As the diagram of pore water pressure along the clay core depends on many variables, its theoretical determination is very complex and imprecise. Ideally, if instrumental measurement data were available, these would be input into the model. However, in absence of measured pore water pressure data, the model proposed by Jimenez et al. (1981) can be applied and pressures at each point can be estimated based upon the limit of the saturation line at the face of the upstream core as shown in Figure 4.
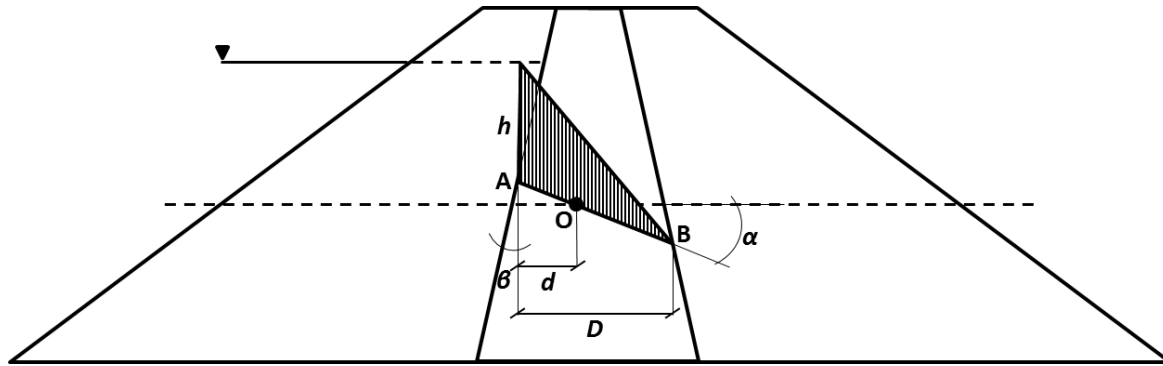

Figure 4: Pore water pressure model proposed by Jimenez et al. (1981).

where:

$$tg\alpha = tg\beta \cdot (k_h/k_v) \tag{2}$$

and the pore water pressure at point "O" is given by:

$$U_o = (1 - d/D) \tag{3}$$

K_h is the horizontal permeability of the clay and K_v the vertical permeability. The total resulting pore pressure is calculated by numerical integration along the surface of the considered potential failure plane. The number of points for the integration is defined by the user. Beyond the three actions described, the core is also subject to a horizontal force produced by the friction of the water along the crest during the overtopping period. This action was considered negligible. All the forces considered by now provoke overturning moment in the upstream-downstream direction, and the horizontal forces can generate shear stress along the potential erosion planes. Conditions for stability can be determined through the interaction of these actions with stabilizing forces.

2.2. Stabilizing Forces

Since the model was developed considering a symmetrical trapezoidal cross-section, one of the stabilizing loads is the weight of the dam. A different density value was established for zones above and within the saturation line. In this analysis, the saturation line is assumed horizontal for simplicity, taking into account the anisotropy of the compacted clay that causes the horizontal permeability to be much higher than the vertical permeability (not uncommonly by an order of 9 times). The weight of the rockfill over the horizontal section evaluated contributes also for static stability. The load generated and the application point depends on the geometry of the dam (Figure 5). Another stabilizing load is the weight of the water over the evaluation plane (Figure 6).
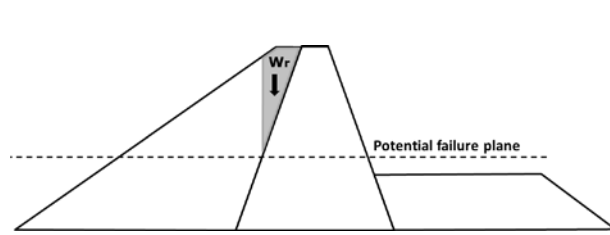

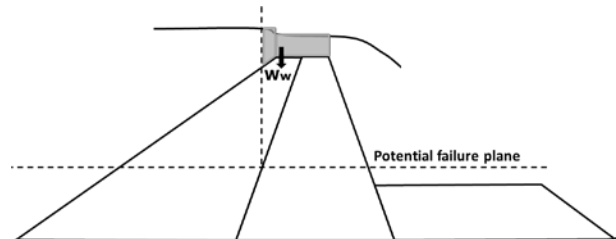Figure 5: Rockfill weight over analyzed plane.

Figure 6: Water weight over analyzed plane.

It was assumed that the forces generated by vertical loads are transferred vertically through the dam body. This hypothesis works well for embankments of infinite length, but a certain error is introduced for real dams of limited length (more significant for narrower dam sites). From this procedure the geometry of the section for each material can be determined, along with its corresponding center of gravity, and consequently the point of load application. In this way, all of the active vertical forces and resulting moments can be determined, all with the downstream-upstream direction. Resistance to sliding is provided by the friction and cohesion forces along the faces of the breach. A rectangular breach was assumed. Width and height of the breach are input for the model. The width should be equal or less than that of the unprotected core. In the unsaturated region of the core the shear resistance can be determined in a trivial way, multiplying the area of the breach faces by the cohesion and summing this with the product of the lateral compression force [N1] the friction angle tangent. Regarding the saturated region, since a short-term and total stress approach was adopted, no friction force was considered. Therefore, the cutting (blocking) force corresponds to the unconsolidated undrained situation (UU) and its value should be determined by the user. If the potential failure plane is in a non-saturated zone, the forces resistant to sliding gain additional support due to the friction at the base of the breach, and the normal force corresponds to the vertical loads.

2.3. Failure Modes

Considering all of the forces involved and their application points, stability conditions can be formulated. Overturning failure occurs if active moment is greater than resistant moment. Sliding failure happens when the total shear resistance in a surface is overcome by the total shear force on that surface. If shear stress induced by the flow on the core surface overcomes a certain critical value, failure happens due to progressive erosion, but this failure mechanism takes a significant period of time, so it is considered that structural failure will occur. However, before sliding or overturning arises, the forces applied to the structure may alter the core, resulting in a rearrangement of

forces. Changes may be caused by excessive tension or compression stresses in the potential failure plane assessed. How these stresses evolve due to the opening of a fissure or the material plasticizing determines the failure mode.

Due to the very low resistance to tension stresses of the clay and materials usually used for the dam core, tension resistance was assumed to be zero. Therefore, if the system of forces causes tension, a fissure opens through the core. It initiates at the most upstream end of the failure plane and progresses downstream. A rearrangement of stresses happens then. The reduction of the effective area of contact on the failure plane results in a concentration of loads, and therefore the increase of the compression stress in the downstream end. Consequently, sliding resistance is diminished since it depends on the product of cohesion and area of contact, and also due to the increase of pore pressure along the fissure. As in the case of a gravity dam, the water penetrates the fissure without significant energy loss in such a way that hydrostatic pressure establishes along the fissure length. This facilitate the fissure progress downstream until the forces system reaches a new equilibrium (Figure 7) or until failure by overturning or sliding occurs.
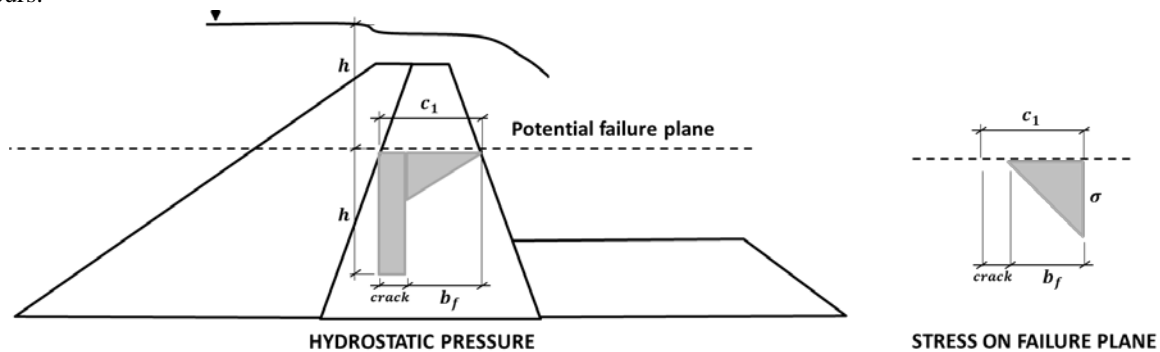
Figure 7: Hydrostatic pressure and stress when fissure is opening.

To assess the stability along the considered potential failure plane, the compressed length (b_f) and the compression stress at the downstream end (σ) must be determined by means of the equilibrium conditions. If the resultant of the actions falls out of the compressed length, overturning is the failure mode. If resultant shear force on the compressed length is greater than the shear resistance due to friction and cohesion, then sliding is the failure mode. If the forces system reaches a new equilibrium situation, but the compression stress (σ) exceeds the limit of the material resistance, plasticizing will occur, and will result in a new configuration of forces that is discussed later.

The pore pressure acting along the compressed length was simplified (Figure 7), in substitution of the model proposed by Jimenez et al. (1981). This simplification does not cause relevant changes in the pore pressure values and has the advantage of simplifying the equations for the crack length assessment.

If the forces applied to the potential failure plane cause a partial plasticizing of the material after the fissure opening, the stress law along the compressed length will be as sketched in Figure 8,a. So the initial assumption about the linear elastic behavior of the material is no longer valid. To verify the stability along the potential failure plane considered, a limit was established for the length of plasticizing (p). This value was determined following the criteria of "plastic yield overturning" laid out in the technical guide for maritime works of the Spanish Government (Soriano, 2005). In order to simplify the mathematical formulations, the model applies just one plasticizing limit, applicable to any potential failure plane of the core.

Depending on the characteristics of the dam and the load state it is possible that in some cases plasticizing may occur without the opening of a fissure. The stress law would then be as sketched in Figure 8,b. Failure criteria for this scenario are analogous to those presented above. It is worth pointing out that the stress distribution can evolve to be the same as that of the case of plasticizing with fissure opening. In both cases, the system of equations necessary to determine the pairs "σ" and "p" or "p" and "b_f" do not allow for an analytical resolution and were solved through optimization methods.
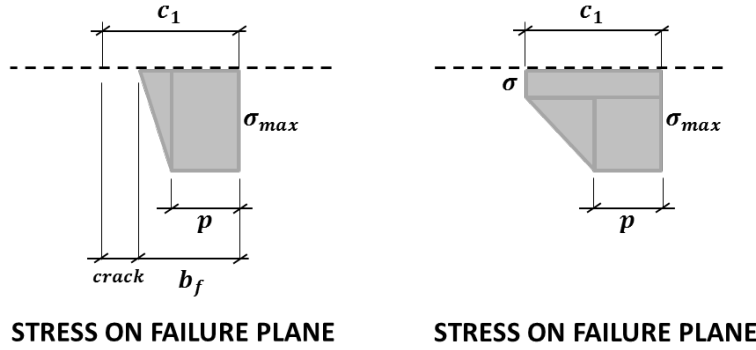
Figure 8: Stress law under partial plasticizing of the section; a) with fissure opening, b) without fissure opening.

3. APPLICATION TO THE TESTED PROTOTYPES

With the objective of evaluating the coherence and applicability of the proposed model, it was decided to simulate the failure of the two prototypes tested in the laboratory by SERPA at the UPM. The results obtained by the model were compared to those obtained from the laboratory experiments. The first of the prototypes tested was a small rockfill dam with central core, 67 cm high, 214 cm wide, with a 14 cm crest. The core was 62 cm high, 20 cm base width and 10 cm crest width (Figure 9). Properties of the materials used in the prototype were inputs for the model (Table 1).
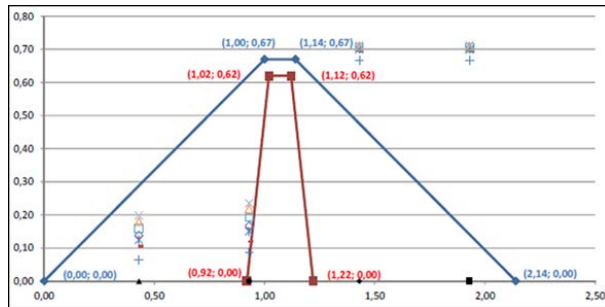

Figure 9: Transverse section of the first prototype tested. Measurements are in meters.
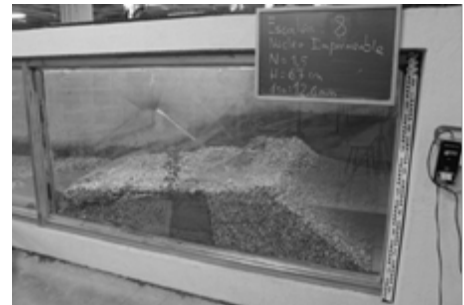

Figure 10: First prototype after failure.

Table 1: Input data for modelling the first prototype tested

MATERIAL PROPERTIES	VALUES	MATERIAL PROPERTIES	VALUES
Reservoir level (m)	0.72	Clay friction angle (°)	25
Breach width (m)	1.32	Clay cohesion (Pa)	50,000
Water density (kg/m³)	1,000	Clay vert. permeability / horizon. permeability	0.11
Gravity (m/s²)	9.81	Clay lateral pressure coefficient	0.7
Rock friction angle (°)	37	Permeability line level (m)	0
Clay density (kg/m³)	1,920	Saturated clay density (kg/m³)	-
Rockfill submerged density (kg/m³)	849	Saturated clay friction angle (°)	-
Compressive strength of clay (Pa)	400,000	Saturated clay cohesion	-

The prototype core was not saturated, so the core did not undergo pore pressure forces. The experiment was, therefore, analogous to a recently constructed dam. Based upon the characteristics in table 1, the model revealed that

the core would fail by overturning, resulting in a 15 cm high breach. The test showed that in fact the failure of the prototype core was indeed by overturning, preceded by a fissure opening without plasticizing, generating a 22 cm high breach (Figure 10) along a slightly inclined plane.

The same proposed model was also used in the analysis of a second tested prototype. The prototype was constructed out of the same materials with the same characteristics as the first, except for the core, which was built with a narrower base, 10 cm width, and was therefore slender. The model predicted a smaller breach, 12cm high, which is in the measured interval of 11 to 14cm. In this case, however, a vertical fissure at the center of the falling piece of clay core was observed prior to the failure.

4. DISCUSSION

It is well known that rocky and clayey materials present a significant dispersion of their properties, and also there are significant uncertainties when trying to quantify them. Therefore, it was convenient to assess, at least in a simplified manner, the sensitivity of the model related to the adopted values for the resistant parameters of the materials. At laboratory size, for the prototype tested, the forces resistant to sliding obtained by the model were around four times the unfavorable actions. Therefore, even if there were great discrepancies in the clay resistance properties (friction angle and cohesion), the failure could never occur by sliding. Therefore, the relevant characteristics for the system of forces under consideration were: density of the clay (ρ_c), density of the submerged rockfill (ρr) and the friction angle of the rockfill (gravel at laboratory size) (φ_r). Each parameter was altered over a wide range, while maintaining the others constant. The height of the breach (h_k) corresponding to each set of parameters is shown in Table 2. None of the involved parameters has a significant impact on the breach height, which remains in a narrow range of values between 14 and 16 cm for the first prototype tested.

Table 2: Breach height as a function of the material properties.

ρ_c (kg/m³)	h_k(m)	ρ_r (kg/m³)	h_k (m)	φ_r (º)	h_k (m)
1700	0.14	700	0.15	20	0.14
1800	0.14	750	0.15	25	0.14
1900	0.15	800	0.15	30	0.14
2000	0.15	850	0.15	35	0.15
2100	0.16	900	0.15	40	0.15
-	-	950	0.15	45	0.15
-	-	1000	0.15	50	0.16
-	-	-	-	55	0.16
-	-	-	-	60	0.16

Particularly, (ρ_r) has a negligible influence in the case under consideration. It makes sense and can be explained. At the same time that the density increases the rockfill pressure, which is a destabilizing force, the rockfill weight increases, which works in an opposite way.

The behavior observed for the clay density (ρ_c) was also as expected: clay weight increase has a stabilizing effect. A greater friction angle of the rockfill reduces the coefficient of the lateral pressure [see Eq. (1)]. Consequently, there is a decrease in the associated overturning force. This situation induces the formation of a failure plane at a lower elevation, given that the destabilizing forces grow more rapidly in depth than stabilizing ones.

The problem is highly conditioned by the geometric dimensions that determine to a large degree the distribution of forces and effects. The height of the water level is the most relevant variable of the model. It determines the hydrostatic pressure, which is the primary active horizontal load, 80% of the total amount in the case of the first prototype. Simultaneous alterations in two or more properties similarly did not provoke significant changes in the height of the breach. Applying a maximum variation (both up and down) of 15% in relation to the amounts showed in Table 2 resulted in a breach height of 0.17 m.

Difference between the breach height predicted by the model and measured in the first prototype tested should mainly be due to the hypotheses adopted for the model. The null resistance to tension hypothesis may be relevant for the explanation of the difference. Since the dam core was partially saturated, the apparent tension resistance due to the negative pore pressure could be relevant at laboratory size, although it is not expected a significant role for a dam of normal size. Another assumption that may partially explain the prediction error is related to the cohesive and friction forces. Given that these forces develop along the horizontal and vertical faces of the breach, each component has a different lever arm. Since the model does not account for deformations, it is not possible to determine at which point of the surface the resisting force is being mobilized. Consequently, there is no way to define an equivalent eccentricity.

In the case under study, shear resistance is developed along the base, so it does not generate moment against overturning. Due to this, a predicted breach height lower than the measured one should be expected. It is still possible that the breach height measurement, done after the conclusion of the experiment, overestimated the breach height value due to structural failure. It is possible that part of the clay core was dragged away after the structural failure. If so, the final height of the standing core would be slightly lower than that caused by overturning, and so a greater height of the breach than that due to the structural failure should be expected.

Agreement between predicted and measured breach height is better for the second prototype tested, which had a more slender clay core. However, the vertical crack observed at the centre of the failed part of the core suggest a different failure mechanism. It is possible that the initiation of the overturning and consequent loss of contact on the horizontal failure plane led to the development of the vertical crack due to the loss of shear resistance in the above mentioned horizontal failure plane. It is not possible to establish general conclusions at this point in the research and more tests are necessary.

5. CONCLUSIONS

A good understanding of the breach formation process is essential to develop a realistic and effective emergency plan. As explained previously, a brittle structural failure may result in a more damaging failure hydrograph than predicted by conventional erosion models. The hypothesis of a gradual failure implies underestimating the flooded areas and the velocity of the flow, and also overestimating the wave propagation time, resulting on the unsafe side. Since flooded area, flow velocity and propagation time are essential parameters for the development of emergency plans, it is relevant that divergence in estimations may reduce the effectiveness of these plans.

It is worth noting that in the case of a structural failure of the dam core both pro- and con- safety factors may not be clear or may be counterintuitive. If material resistance is underestimated or the core is thinner, an earlier failure would be predicted, but the failure hydrograph would be less damaging than that for a more resistant material or thicker core. On the other hand, overestimating the material strength, or a thicker core, would result in a later but higher breach and a more damaging failure hydrograph, with a greater time period between the beginning of the overtopping and the reservoir water release. It would also be possible as an extreme case that the core could resist without failure. Therefore, it is desirable to predict an envelope of possible scenarios and to determine a range of probable values for the breach height, to inform decision making in overtopping situation.

Bearing in mind the complexity of the addressed problem and the promising results obtained with the simple model developed, a more detailed model will be undertaken, eliminating some simplifications and adding other types of failures like structural breakage with vertical fissure and non-horizontal sliding.

6. REFERENCES

ASCE/EWRI Task Committee on Dam/Levee Breaching (2011). "Earthen Embankment Breaching." *J. Hydraul. Eng.*, 10.1061/(ASCE)HY.1943-7900.0000498, 1549-1564.

Broich, K. (2005). "Breach modelling: Description of breach model DEICH_P." <http://www.impact-project.net/AnnexII_DetailedTechnicalReports/AnnexII_PartA_WP2/IMPACT-36Month_Report-UniBwM-wp23-appendix-1-1_description.pdf> (May, 28, 2016).

Odendaal, W., & Van Zyl, F. C. (1979). Failure of a cofferdam due to overtopping. In XII ICOLD Congress on Large Dams, Q (Vol. 49, pp. 141-156).

Salas, J., Jimenez, A., Alpañes, J. L. and Serrano, A. A. (1981). Geotechnical and Foundation. Volume I to III. 2nd Edition, Rueda, Madrid (in Spanish).

Soriano, A. (2005). In Ministry of Development: State Ports Authority (Ed.), Geotechnical recommendations for maritime and ports projects (in Spanish).

Toledo, M. A. (1997). "Embankment dams slip failure due to overtopping". XIX International Congress on Large Dams, ICOLD, Florence, Italy., 317-330.

Toledo, M. A., Alves R. M., and Morán, R. (2015). "Structural failure of the clay core or the upstream face or rockfill dams in overtopping scenario". Proc., 1st International Seminar on Dam Protections Against Overtopping and Accidental Leakage", UPM, Madrid, Spain., 101-109.